

Supplementary Material to the Paper

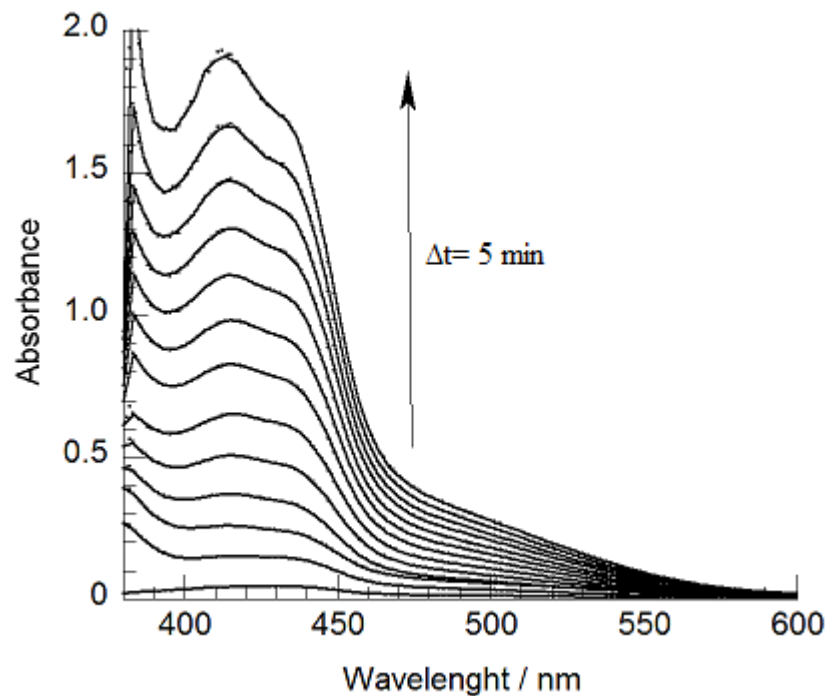
Oxidation of 3,5-di-*tert*-butylcatechol and 2-aminophenol by molecular oxygen catalyzed by an organocatalyst†

Gábor Székely, Nárcisz Bagi, József Kaizer* and Gábor Speier*

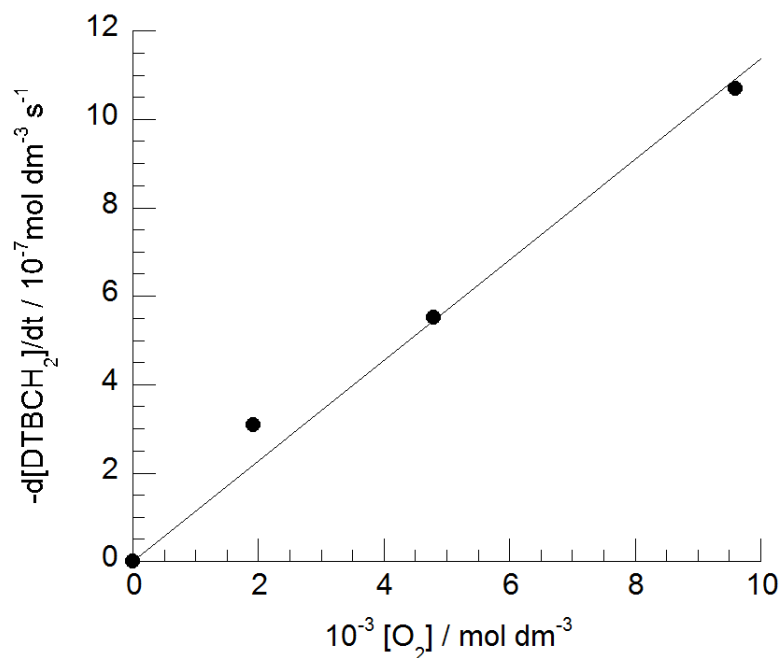
List of content:

Page

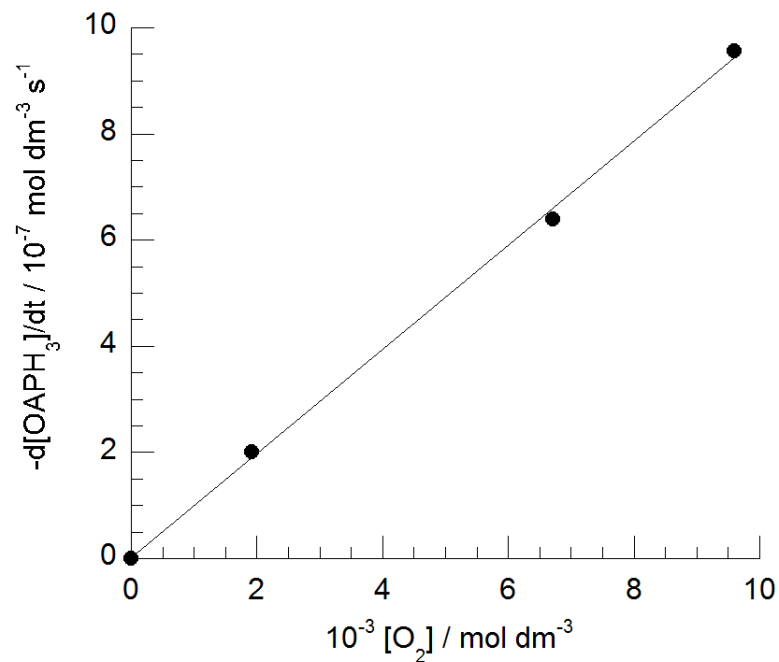
SFigure 1. The catalytic oxidation of OAPH ₃ followed by UV-vis spectroscopy	S2
SFigure 2. Plot of oxidation of DTBCH ₂ versus dioxygen concentration	S3
SFigure 3. Plot of oxidation of OAPH ₃ versus dioxygen concentration	S4
SFigure 4. The dependence of reaction rate of the oxidation of DTBCH ₂ on the catalyst concentration	S5
SFigure 5. The dependence of reaction rate of the oxidation of OAPH ₃ on the catalyst concentration	S6
SFigure 6. Time course of the oxidation of OAPH ₃	S7
SFigure 7. Rate dependence of the oxidation of DTBCH ₂ on the initial concentration of DTBCH ₂	S8
SFigure 8. Rate dependence of the oxidation of OAPH ₃ on the initial concentration of OAPH ₃	S9
SFigure 9. The Arrhenius plot on the oxidation of DTBCH ₂	S10
SFigure 10. The Arrhenius plot on the oxidation of OAPH ₃	S11
SFigure 11. The Kinetic Isotope Effect of DTBCH ₂	S12
SFigure 12. The Kinetic Isotope Effect of OAPH ₃	S13
STable 1. The kinetic data of the catalytic oxidation of DTBCH ₂	S14
STable 2. The kinetic data of the catalytic oxidation of OAPH ₃	S15
Experiments details	S16
SFigure 13. ¹ H NMR spectrum of 3,5-di- <i>tert</i> -butylquinone.	S17
SFigure 14. ¹³ C NMR spectrum of 3,5-di- <i>tert</i> -butylquinone.	S18
SFigure 15. ¹ H NMR spectrum of 2-aminophenoxyazin-3-one.	S19
SFigure 16. ¹³ C NMR spectrum of 2-aminophenoxyazin-3-one.	S20
SFigure 17. Mass spectrum of 3,5-di- <i>tert</i> -butylquinone.	S21
SFigure 18. Mass spectrum of 2-aminophenoxyazine-3-one.	S22



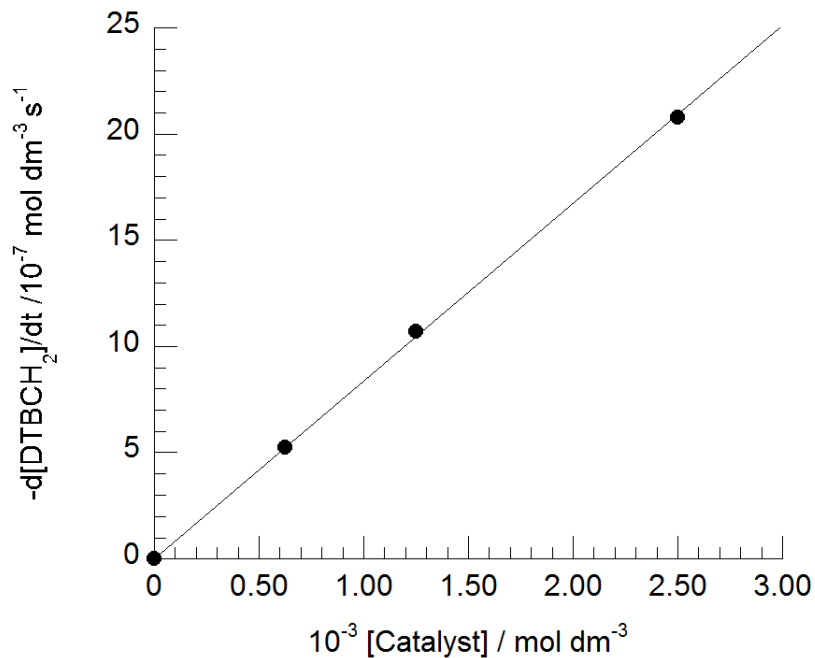
SFigure 1. The catalytic oxidation of OAPH₃ followed by UV-vis spectroscopy.
[OAPH₃] = 11.25 × 10⁻² M, [1,3,2-oxazaphosphole] = 1.25 × 10⁻³ M,
[O₂] = 9.5 × 10⁻³ M, T = 298.15 K, 20 mL MeOH.



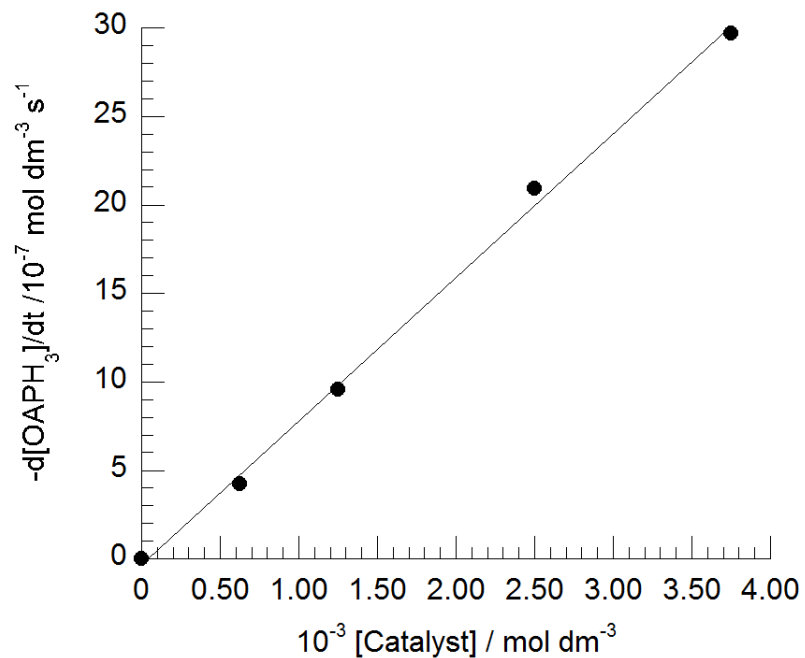
SFigure 2. Plot of oxidation of DTBCH_2 versus dioxygen concentration. $[\text{DTBCH}_2] = 12.5 \times 10^{-2} \text{ M}$, $[1,3,2\text{-oxazaphosphole}] = 1.25 \times 10^{-3} \text{ M}$, $T = 298.15 \text{ K}$, 10 mL MeOH.



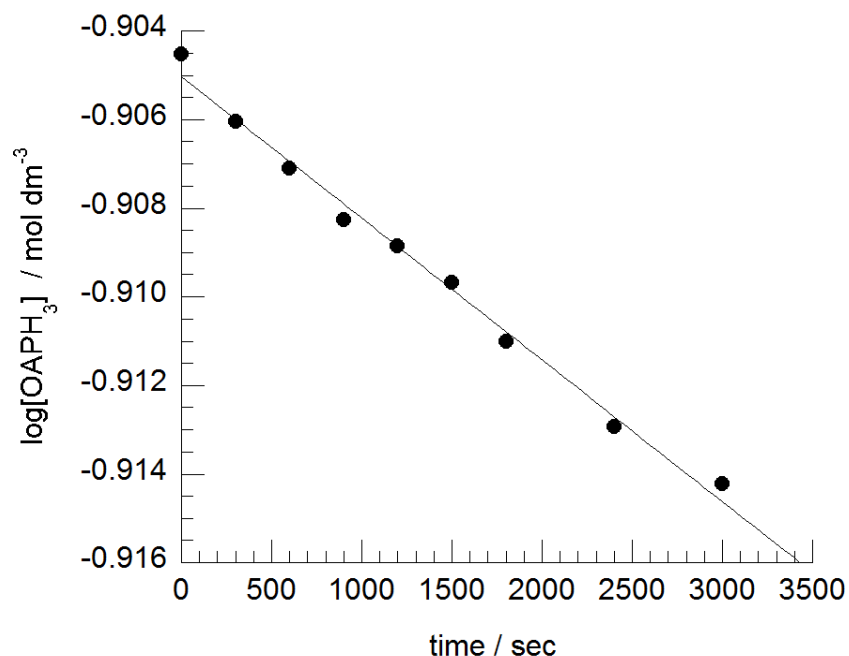
SFigure 3. Plot of oxidation of OAPH₃ versus dioxygen concentration. [OAPH₃] = 12.5×10^{-2} M, [1,3,2-oxazaphosphole] = 1.25×10^{-3} M, T = 298.15 K, 20 mL MeOH.



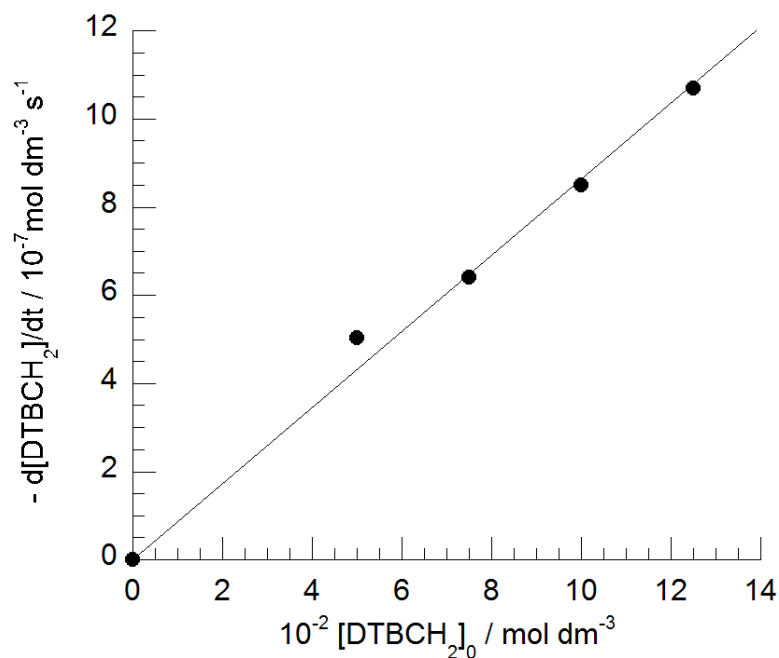
SFigure 4. The dependence of reaction rate of the oxidation of DTBCH₂ on the catalyst concentration. [DTBCH₂] = 12.5 × 10⁻² M, [O₂] = 9.5 × 10⁻³ M, T = 298.15 K, 10 mL MeOH.



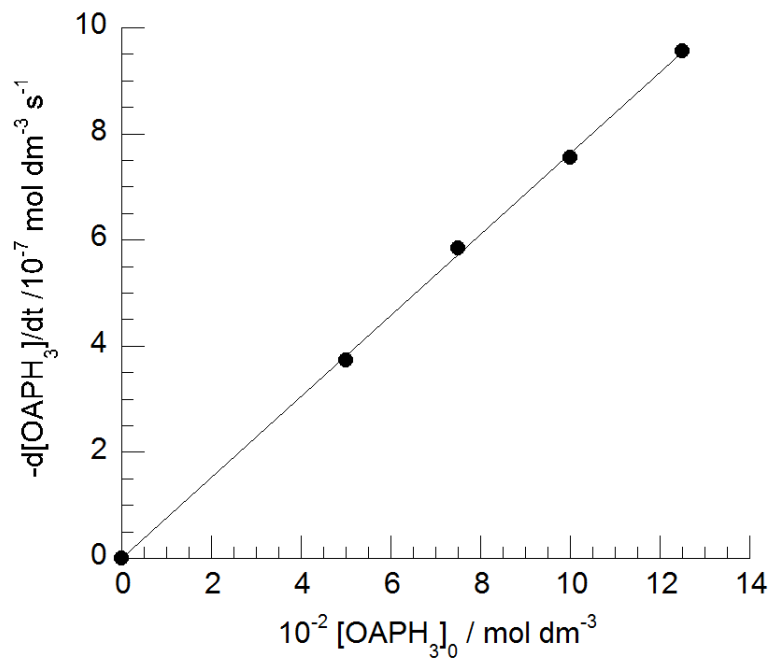
SFigure 5. The dependence of reaction rate of the oxidation of OAPH₃ on the catalyst concentration. [OAPH₃] = 12.5 × 10⁻² M, [O₂] = 9.5 × 10⁻³ M, T = 298.15 K, 20 mL MeOH.



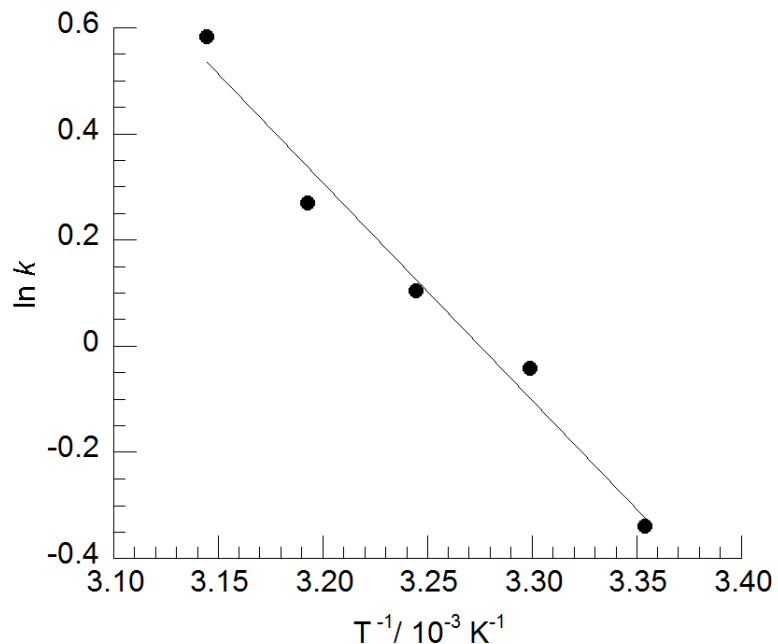
SFigure 6. Time course of the oxidation of OAPH₃. [OAPH₃] = 12.5 × 10⁻² M, [1,3,2-oxazaphosphole] = 1.25×10⁻³, [O₂] = 9.5 × 10⁻³ M, T = 298.15 K, 20 mL MeOH.



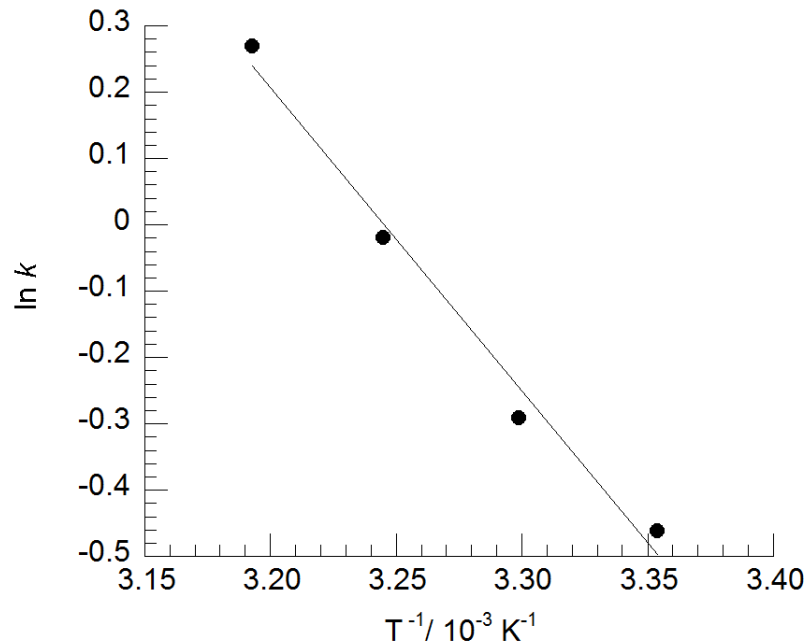
SFigure 7. Rate dependence of the oxidation of DTBCH₂ on the initial concentration of DTBCH₂. [1,3,2-oxazaphosphole] = 1.25×10^{-3} M, [O₂] = 9.5×10^{-3} M, T = 298.15 K, 10 mL MeOH.



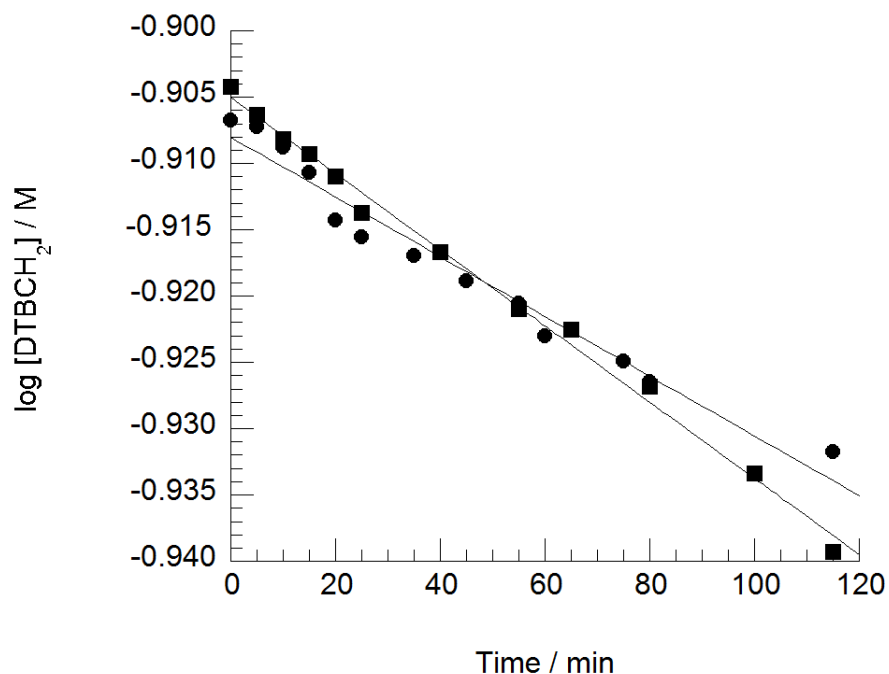
SFigure 8. Rate dependence of the oxidation of OAPH₃ on the initial concentration of OAPH₃. [1,3,2-oxazaphosphole] = 1.25×10^{-3} M, [O₂] = 9.5×10^{-3} M, T = 298.15 K, 20 mL MeOH.



SFigure 9. The Arrhenius plot on the oxidation of DTBCH_2 .



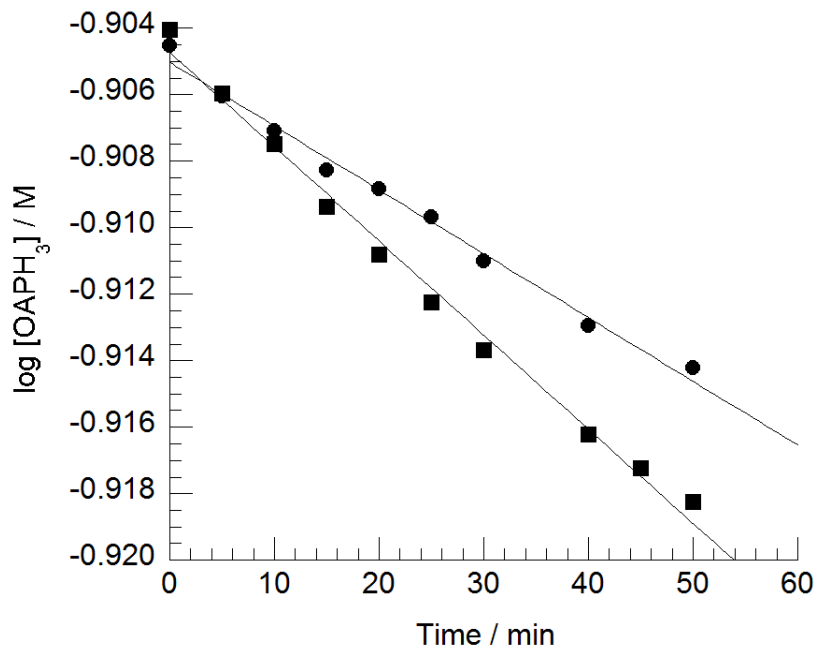
SFigure 10. The Arrhenius plot on the oxidation of OAPH₃.



SFigure 11. The Kinetic Isotope Effect data of DTBCH₂.

(■ in MeOH, • in MeOD)

[DTBCH₂] = 12.5 × 10⁻² M, [1,3,2-oxazaphosphole] = 1.25×10⁻³, [O₂] = 9.5 × 10⁻³ M,
T = 298.15 K, 10 mL MeOD/MeOH.



SFigure 12. The Kinetic Isotope Effect data of OAPH₃.

(■ in MeOH, • in MeOD)

[OAPH₃] = 12.5 × 10⁻² M, [1,3,2-oxazaphosphole] = 1.25 × 10⁻³, [O₂] = 9.5 × 10⁻³ M,
T = 298.15 K, 20 mL MeOD/MeOH.

STable 1. The kinetic data of the catalytic oxidation of DTBCH₂.

Entry	Temp. (°C)	[O ₂] (10 ⁻³ mol dm ⁻³)	[1,3,2- oxazaphosphole] (10 ⁻³ mol dm ⁻³)	[DTBCH ₂] (10 ⁻² mol dm ⁻³)	-d[DTBCH ₂]/dt (10 ⁻⁷ Ms ⁻¹)	k _{obs} (M ⁻² s ⁻¹)
1.	25	9.50	1.25	5.00	5.02 ± 0.30	0.84±0.08
2.	25	9.50	1.25	7.50	6.41 ± 0.17	0.71±0.09
3.	25	9.50	1.25	10.00	8.49 ± 0.03	0.70±0.09
4.	25	9.50	1.25	12.50	10.69 ±0.24	0.71±0.09
5.	25	9.50	0.625	12.50	5.25 ± 0.27	0.70±0.09
6.	25	9.50	2.500	12.50	20.80 ± 0.24	0.69±0.09
7. *	25	1.92	1.25	12.50	3.08 ± 0.12	1.03±0.10
8.	25	4.80	1.25	12.50	5.52 ± 0.25	0.74±0.09
					avg.:0.76±0.11	
9.	30	9.48	1.25	12.50	14.20 ± 0.57	0.96±0.10
10.	35	9.46	1.25	12.50	16.40 ± 0.78	1.11±0.11
11.	40	9.44	1.25	12.50	19.32 ± 1.07	1.31±0.11
12.	45	9.42	1.25	12.50	24.40 ± 1.55	1.79±0.11
13.	25	9.50	1.25	12.50	10.20 ± 0.22	0.69±0.09

Mean value of the kinetic constant k_{obs} and its standard deviations σ(k_{obs}) were calculated as

$$k_{\text{obs}} = (\sum_i w_i k_i / \sum_i w_i) \text{ and } \sigma(k_{\text{obs}}) = (\sum_i w_i (k_i - k_{\text{avg}})^2 / (n-1) \sum_i w_i)^{1/2}, \text{ where } w_i = 1/\sigma^2_i$$

* Under air

13. in MeOD

STable 2. The kinetic data of the catalytic oxidation of OAPH₃.

Entry	Temp. (°C)	[O ₂] (10 ⁻³ mol dm ⁻³)	[1,3,2- oxazaphosphole] (10 ⁻³ mol dm ⁻³)	[OAPH ₃] (10 ⁻² mol dm ⁻³)	d[OAPH ₃]/dt (10 ⁻⁷ Ms ⁻¹)	k _{obs} (M ⁻² s ⁻¹)
1.	25	9.50	1.25	5.00	3.73 ± 0.25	0.61±0.03
2.	25	9.50	1.25	7.50	5.85 ± 0.18	0.63±0.03
3.	25	9.50	1.25	10.00	7.56 ± 0.12	0.62±0.03
4.	25	9.50	1.25	12.50	9.56 ± 0.10	0.62±0.03
5.	25	9.50	0.63	12.50	4.26 ± 0.23	0.55±0.03
6.	25	9.50	2.50	12.50	20.90 ± 0.35	0.68±0.04
7.	25	9.50	3.75	12.50	29.70 ± 0.65	0.65±0.04
8. *	25	1.92	1.25	12.50	2.00 ± 0.32	0.65±0.04
9.	25	6.72	1.25	12.50	6.40 ± 0.16	0.59±0.03
					avg.:0.62±0.03	
10.	25	9.50	1.25	12.50	9.56 ± 0.10	0.62±0.03
11.	30	9.48	1.25	12.50	11.25 ± 0.10	0.75±0.03
12.	35	9.46	1.25	12.50	14.70 ± 0.13	0.98±0.04
13.	40	9.44	1.25	12.50	19.50 ± 0.29	1.31±0.04
14.	25	9.50	1.25	12.50	6.53 ± 0.10	0.44±0.02

Mean value of the kinetic constant k_{obs} and its standard deviations σ(k_{obs}) were calculated as

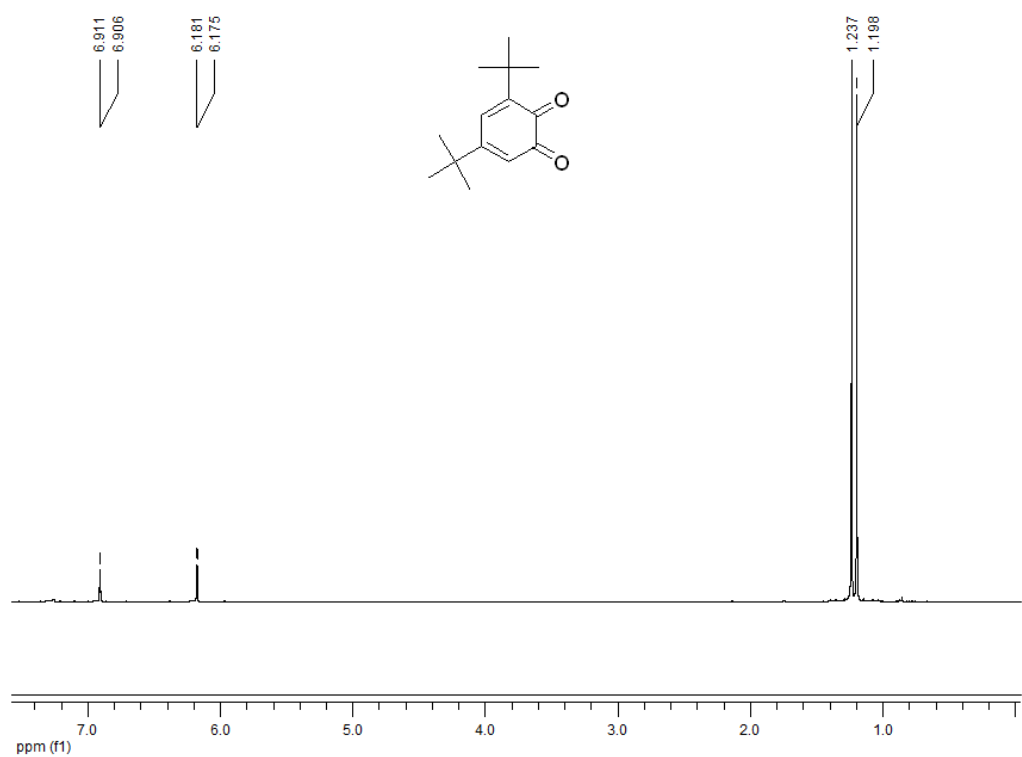
$$k_{\text{obs}} = (\sum_i w_i k_i / \sum_i w_i) \text{ and } \sigma(k_{\text{obs}}) = (\sum_i w_i (k_i - k_{\text{avg}})^2 / (n-1) \sum_i w_i)^{1/2}, \text{ where } w_i = 1/\sigma^2_i$$

* Under air

14. in MeOD

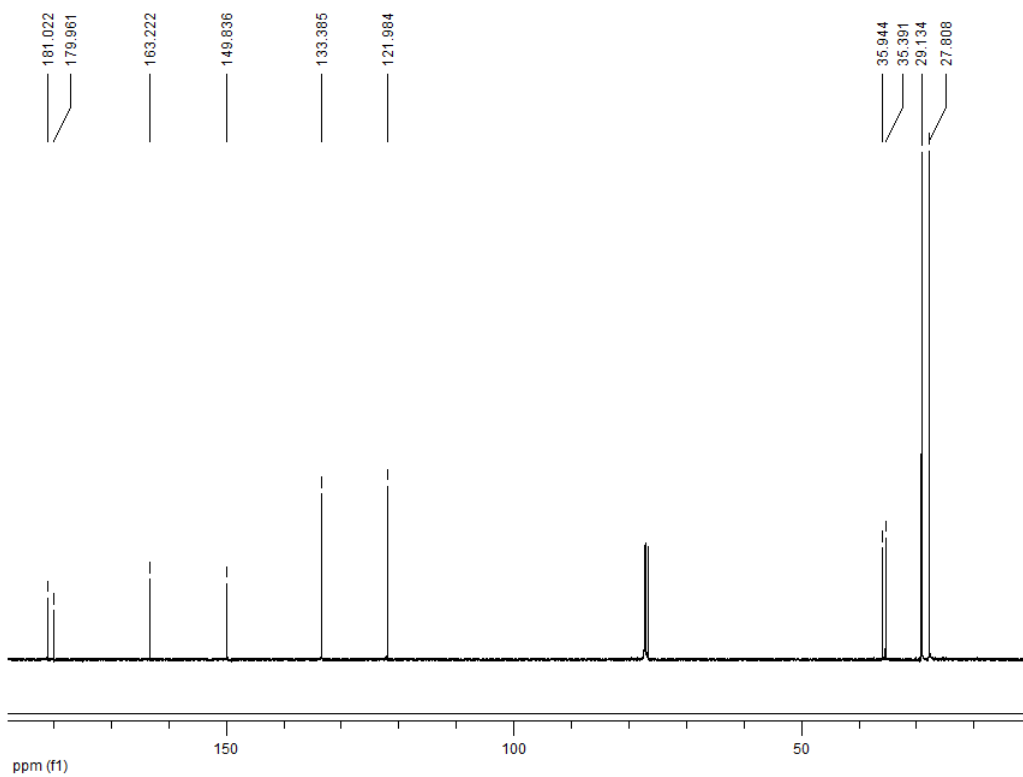
Experiments details

Instruments: Gas chromatographic – Mass Spectrometric (GC-MS) analyses were carried out on a GCMS-QP2010 SE instrument with secondary electron multiplier detector. NMR spectrum: ^1H and ^{13}C NMR spectra were collected on 400 MHz NMR spectrometers (Bruker Avance) using DMSO-d₆ and CDCl₃ as solvent. Chemical shifts are reported in parts per million (ppm). Chemical shifts for protons are reported in parts per million downfield and are referenced to residual protium in the NMR solvent (δ (DMSO-d₆) = 2.50, 39.52 and δ (CDCl₃) = 7.24, 77)).



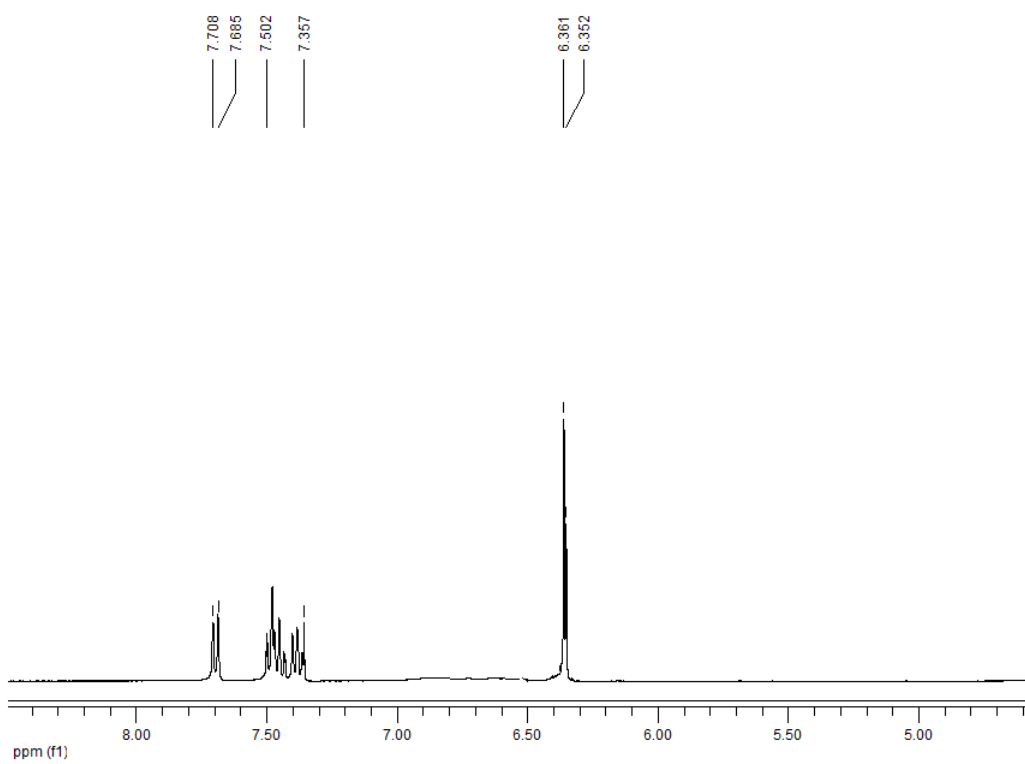
SFigure 13. ¹H NMR spectrum of 3,5-di-*tert*-butylquinone.

(Uyanik, M.; Mutsuga, T.; Ishihara, K. *Molecules* **2012**, *17*, 8604–8616.)



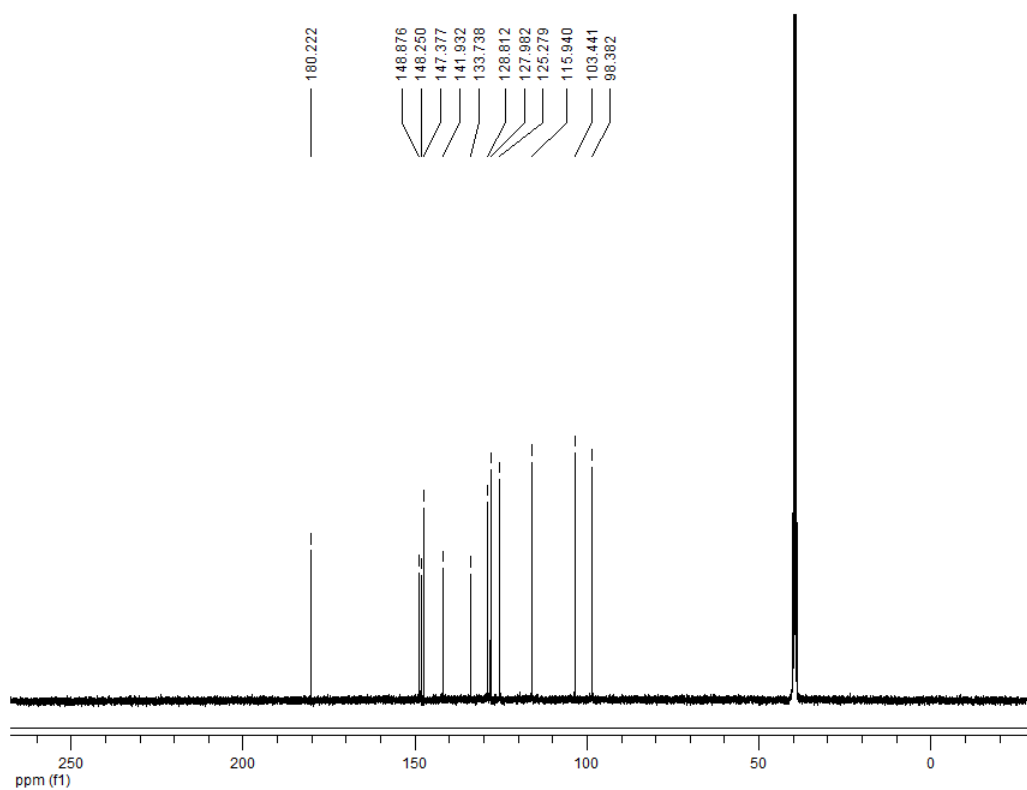
SFigure 14. ¹³C NMR spectrum of 3,5-di-*tert*-butylquinone.

(Uyanik, M.; Mutsuga, T.; Ishihara, K. *Molecules* **2012**, *17*, 8604-8616.)



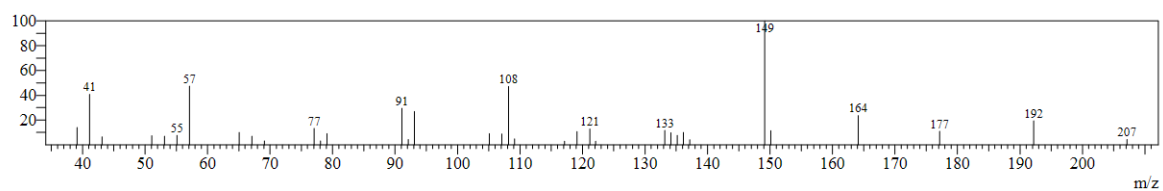
SFigure 15. ^1H NMR spectrum of 2-aminophenoxazine-3-one.

(Suzuki, H., Furusko, Y., Higashi, T., Ohnishi, Y., Horinouchi, S. *J. Biol. Chem.* **2006**, 281, 824-833.)



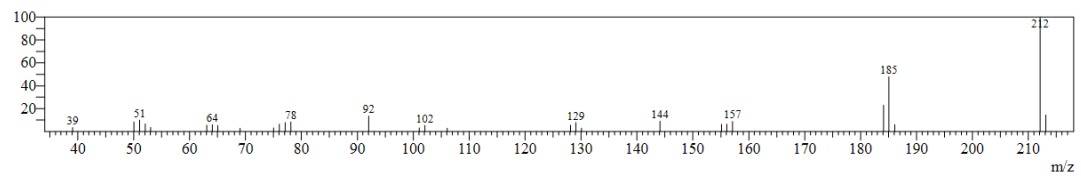
SFigure 16. ^{13}C NMR spectrum of 2-aminophenoxazine-3-one.

(Suzuki, H., Furusko, Y., Higashi, T. Ohnishi, Y., Horinouchi, S. *J. Biol. Chem.* **2006**, 2, 824-833.)



SFigure 17. Mass spectrum of 3,5-di-*tert*-butylquinone.

(http://sdbs.db.aist.go.jp/sdbs/cgi-bin/direct_frame_top.cgi)



SFigure 18. Mass spectrum of 2-aminophenoxyazine-3-one.

(Friebe, A., Vilich, V., Hennig L., Kluge M., Sicker D. *Appl Environ Microbiol.* **1998**, *64*(7), 2386–2391.)